

See discussions, stats, and author profiles for this publication at: <https://www.researchgate.net/publication/262023021>

# Allosteric Transition Induced by Mg<sup>2+</sup> Ion in a Transactivator Monitored by SERS

ARTICLE *in* THE JOURNAL OF PHYSICAL CHEMISTRY B · MAY 2014

Impact Factor: 3.3 · DOI: 10.1021/jp5000733 · Source: PubMed

---

CITATIONS

4

READS

44

## 6 AUTHORS, INCLUDING:



Partha P. Kundu

M. S. Ramaiah University of Applied Sciences

8 PUBLICATIONS 15 CITATIONS

[SEE PROFILE](#)



Ganduri Swapna

7 PUBLICATIONS 29 CITATIONS

[SEE PROFILE](#)



Valakunja Nagaraja

Indian Institute of Science

163 PUBLICATIONS 2,720 CITATIONS

[SEE PROFILE](#)



Chandrabhas Narayana

Jawaharlal Nehru Centre for Advanced Scienti...

155 PUBLICATIONS 1,714 CITATIONS

[SEE PROFILE](#)

# Allosteric Transition Induced by Mg<sup>2+</sup> Ion in a Transactivator Monitored by SERS

Partha P. Kundu,<sup>†,⊥</sup> Tuhin Bhowmick,<sup>‡,⊥</sup> Ganduri Swapna,<sup>§</sup> G. V. Pavan Kumar,<sup>†,||</sup> Valakunja Nagaraja,<sup>\*,§</sup> and Chandrabhas Narayana<sup>\*,†</sup>

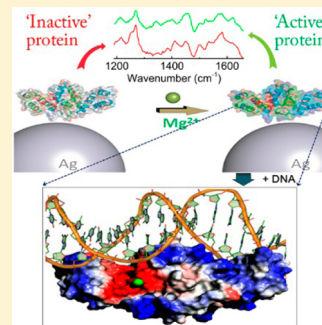
<sup>†</sup>Light Scattering Laboratory, Chemistry and Physics of Material Unit, Jawaharlal Nehru Center for Advanced Scientific Research, Jakkur, Bangalore 560064, India

<sup>‡</sup>Department of Physics, Indian Institute of Science, Bangalore 560012, India

<sup>§</sup>Department of Microbiology and Cell Biology, Indian Institute of Science, Bangalore 560012, India

## S Supporting Information

**ABSTRACT:** We demonstrate the utility of the surface-enhanced Raman spectroscopy (SERS) to monitor conformational transitions in protein upon ligand binding. The changes in protein's secondary and tertiary structures were monitored using amide and aliphatic/aromatic side chain vibrations. Changes in these bands are suggestive of the stabilization of the secondary and tertiary structure of transcription activator protein C in the presence of Mg<sup>2+</sup> ion, whereas the spectral fingerprint remained unaltered in the case of a mutant protein, defective in Mg<sup>2+</sup> binding. The importance of the acidic residues in Mg<sup>2+</sup> binding, which triggers an overall allosteric transition in the protein, is visualized in the molecular model. The present study thus opens up avenues toward the application of SERS as a potential tool for gaining structural insights into the changes occurring during conformational transitions in proteins.



## INTRODUCTION

Vibrational spectroscopy is a powerful tool for studying biomolecules as it provides detailed information on the molecular structure and intermolecular interactions. Moreover, the technique can be applied regardless of the state of the system allowing it to be probed close to the physiological condition. Raman and IR are two main techniques in vibrational spectroscopy. Although IR spectroscopy is a very useful technique, one of the major problems with this technique is the interference from the water bands in the region of interest.<sup>1</sup> However, the problem can be overcome by reducing the path length or using attenuated total reflection (ATR) method,<sup>2</sup> but in both cases, short penetration depth is known to affect the sensitivity.<sup>3</sup> In contrast, the Raman spectroscopy is devoid of this problem, but the weak scattered signal poses some limitations to its use. Ultraviolet resonance Raman spectroscopy (UVRR) enhances the signal by 10<sup>4</sup> times over the normal Raman. However, the high energy UV photons may cause photochemical damage to the sample.<sup>4</sup> Surface-enhanced Raman scattering (SERS) is an alternative technique that uses the plasmon resonance of noble metal nanoparticles or nanoscale surface structures to increase the Raman signal from analytes up to the order of 10<sup>14</sup>.<sup>5</sup> Hence, SERS requires less laser power, low concentration of the sample, and shorter acquisition time. The strong enhancement of the Raman signal has made it possible to study, in some cases, single molecule through SERS, with no parallel from the other vibrational techniques mentioned above.<sup>5–8</sup> Lower detection limits, narrow spectral bandwidths, and the capacity to be used with or without optical labels have made SERS a good choice for

various biological applications.<sup>9–22</sup> Many studies have reported label-free protein detection using SERS.<sup>23–26</sup> In this work, we have evaluated the utility of SERS to probe conformational transitions occurring in protein upon ligand binding, using a well characterized system. C protein, a transcriptional activator, required for the activation of bacteriophage Mu late genes during the lytic cycle of the phage is used for the present analysis. The protein is dependent on Mg<sup>2+</sup> for its DNA binding and transactivation.<sup>27,28</sup> Although studies on conformational changes of proteins by means of Raman spectroscopy has been reported in literature,<sup>29–37</sup> SERS has been mainly restricted as a sensitive detection method for quantitative analysis rather than structural analysis.<sup>38,39</sup> To the best of our knowledge, very few attempts have been made to probe conformational changes using SERS.<sup>23,39,40</sup> Here, we have carried out a comprehensive SERS study to trace both local and overall conformational changes in this transcriptional activator C.

## EXPERIMENTAL DETAILS

**Protein Purification.** C protein and its mutants were purified from *E. coli* BL26 (DE3) carrying plasmid pVR7 or pVNC4 by following the procedure described earlier.<sup>41</sup> The purified protein was dialyzed against HEPES buffer containing EDTA [10 mM HEPES (pH 7.6), 50 mM NaCl, and 20 mM EDTA] for 1 h at 4 °C to chelate out the intrinsically bound Mg<sup>2+</sup>.

**Received:** January 3, 2014

**Revised:** April 30, 2014

**Published:** May 2, 2014

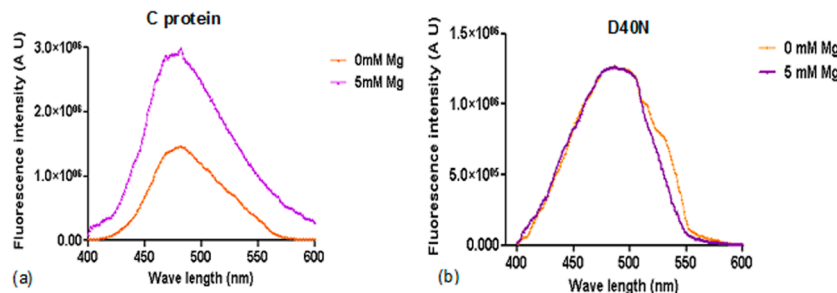


**Figure 1.**  $Mg^{2+}$ -induced conformational changes in C protein. Tertiary structural changes were monitored by recording fluorescence emission spectra in the presence of extrinsic fluoro ANS as described in experimental details. Background corrected fluorescence spectra of (a) C protein and (b) mutant D40N in the absence (0 mM) and presence (5 mM) of  $MgCl_2$ .

Further, dialysis was continued in HEPES buffer without EDTA for 2 h, with a buffer change after 1 h. Dialyzed protein was quantified using the Bradford assay and used for SERS analysis.

**ANS Fluorescence.** Fluorescence emission spectra were recorded on a Jobin-Yvon fluorometer FluoroMax3, thermostated at 25 °C. EDTA treated C protein/mutant D40N (1  $\mu$ M concentration) was incubated both in the absence and presence of 5 mM  $Mg^{2+}$  for 15 min at 25 °C. One hundred micromolar 8-anilino naphthalene-1-sulfonic acid (ANS) dye was added as extrinsic fluor to 1  $\mu$ M protein in Tris pH 7.5 buffer to prepare samples for emission spectra. Next, the samples were subjected to excitation at 360 nm, and emission values were integrated between 400 and 600 nm. All the fluorescence emission spectra and fluorescence intensities were corrected for buffer,  $Mg^{2+}$ , and ANS intrinsic fluorescence.

**Silver Colloid Preparation.** The Ag solution was prepared by method of Lee and Meisel.<sup>42</sup> Forty-five milligrams of  $AgNO_3$  was dissolved in 250 mL of water, and the solution was brought to the boil. Next, a solution of 1% sodium citrate (5 mL) was added under vigorous stirring, and boiling was continued for 60 min. The plasmon absorption maximum was located at 410 nm (see Supporting Information, Figure S1) confirming the expected behavior of the nanoparticles. The size of the nanoparticle was confirmed by TEM image and DLS measurement (see Supporting Information, Figure S1).

**SERS Measurements.** SERS spectra of C protein was recorded in the 180° backscattering geometry using 632.8 nm He–Ne laser (model 30995, Research Electro Optics, Inc., U.S.A.) as a Raman excitation source. The spectrometer consists of a monochromator (Horiba Jobin-Yvon, iHR 320) and a Peltier-cooled charge-coupled device (CCD) (AndoriDus).<sup>43</sup> A holographic with 1800 grooves  $mm^{-1}$  grating was used along with the 200  $\mu$ m spectrograph entrance slit setting, providing  $\sim 3$   $cm^{-1}$  resolution. For SERS studies of protein, a 60× infinity-corrected objective (Nikon Plan Apo, Japan, NA 0.9) was used. The laser power used at the sample was 6 mW. The average accumulation time used was 180 s. SERS spectra shown in Figures 4 and 5 were background corrected and smoothed using 5 point FFT filter technique Origin software. All analyses (band position and intensity) have been performed by first smoothing the spectra using 15 point FFT filter technique and then taking the second derivative of the spectra (not shown).

C protein solution (140 ng/ $\mu$ L) was mixed with colloidal Ag solution in the ratio 1:10 (v/v) and kept for 5 min for adsorption of protein on the nanoparticles. Ten microliters of mixture solution was then drop-coated over a siliconized, hydrophobic glass cover slide (Hampton Research CAT NO HR3-223). The spectra were taken in the liquid form by focusing the objective

inside the drop. The hydrophobic surface prevents the drop from flattening, reducing the amount of solution required, which is especially useful when the quantity of sample available is very small. For studying the effect of  $Mg^{2+}$ , the protein (140 ng/ $\mu$ L) was incubated for 15 min with 5 mM  $Mg^{2+}$  prior to the addition of Ag solution.

Details of computational methodologies for modeling of C protein are provided in the Supporting Information.

## RESULTS AND DISCUSSION

The transactivator protein C is a dimer<sup>44</sup> that binds dyad-symmetry element upstream, overlapping the –35 region of the target promoters.<sup>45</sup> Although crystal or solution structure of C protein is not reported, circular dichroism (CD) and fluorescence studies showed secondary and tertiary structural changes in C protein upon the addition of  $Mg^{2+}$ .<sup>27,28</sup> Hydrophobic reporter dye ANS used in fluorescence emission spectroscopy of the wild-type C protein exhibited a blue shift in the emission maxima with an enhancement in fluorescence intensity upon binding to the buried hydrophobic sites of the protein (Figure 1). Enhanced fluorescence intensity seen with the protein upon the addition of  $Mg^{2+}$ , indicated gross tertiary structural changes in the protein (Figure 1a). Previous studies<sup>28</sup> also indicated a  $Mg^{2+}$  coordinating motif in the protein, consisting of an acidic residue patch, rich in Asp and Glu. Mutation in one of the key residues D40 affected  $Mg^{2+}$  binding, leading to a decreased DNA binding and reduction in the level of transcription activation. Unlike the wild-type C protein, ANS signal from the mutant D40N showed no response to the addition of the metal ion (Figure 1b).

In order to get an atomic level understanding of the structural transitions, we have employed SERS, which has all the advantages of the vibrational techniques, but with greater sensitivity. The well-established marker bands in Raman spectroscopy were used in our SERS based studies. We have also taken into account the properties of SERS that are different from normal Raman in terms of selection rule and distance dependency. Unlike normal Raman spectra, where the spectral contributions arise from all the amino acids of the protein, SERS spectra spectral contributions, in general, are due to those amino acids that are having higher electronic polarizability and are close to the metal surface. Contributions from amino acids located far away from the metal surface is negligible to the spectra since the electromagnetic enhancement factor falls off rapidly with the distance of the molecule from the metal surface,<sup>46</sup> at a rate of  $1/r^2$ , where  $r$  = distance from metal surface. This seems to be a limitation of the technique, as (a) the protein should be adsorbed onto the metal surface and (b) interpretation can be made from

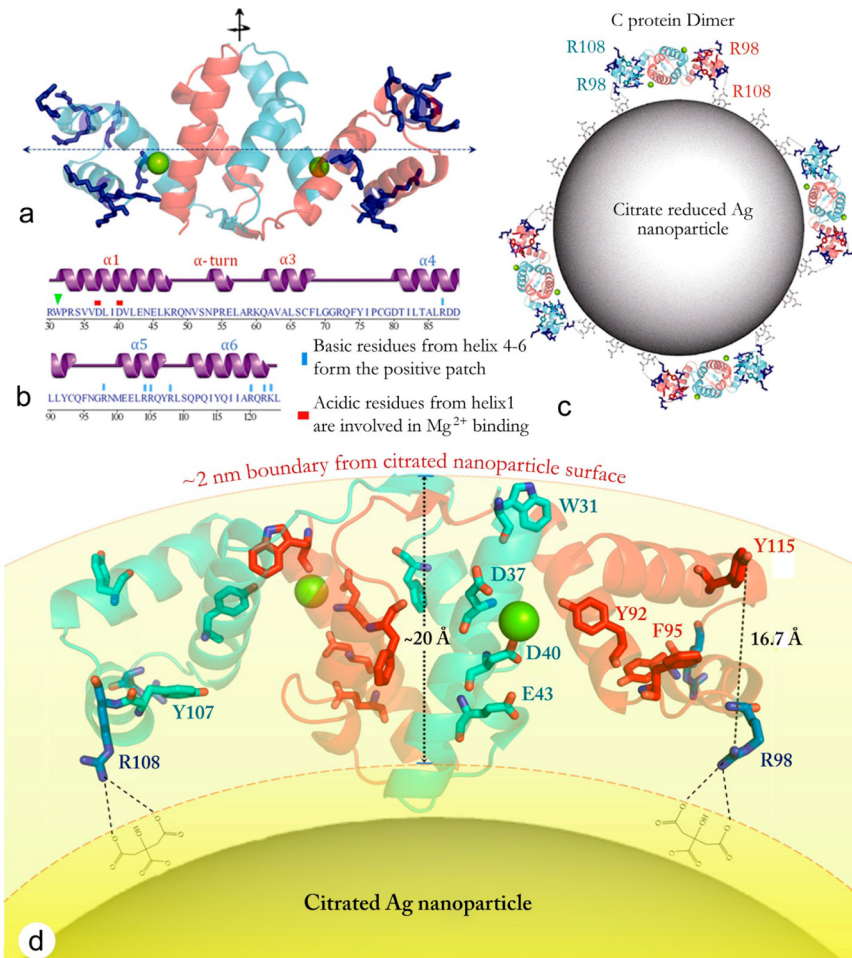


**Figure 2.** Positively charged patches on C protein surface and C's possible mode of interaction with silver nanoparticle. (a) Positively charged Arg and Lys from helix 4 to helix 6 of each monomer in stick representation. The dotted line represents the long axis of C dimer, perpendicular to the 2-fold symmetry axis of dimerization. (b) The blue blocks highlight the position of positively charged patches, consisting of basic amino acid residues, such as R87, 98, 104, 105, 108, 120, 122, and K123 from each monomer, mapped on a secondary structural representation of C protein. To elucidate the relative location of the acidic patch involved in  $Mg^{2+}$  ion binding, D37 and D40 from helix 1 are also marked by red blocks. The green triangle marks the position of W31 at loop-helix 1 boundary. (c) Possible mode of interaction of C protein dimers to the surface of citrate-reduced Ag nanoparticles, using the positively charged patches described in panel a. (d) The region of C protein within the vicinity ( $\sim 2$  nm) of the citrated silver nanoparticle surface. Various aromatic residues, such as W31, Y92, 107, 115, F68, and 95 along with acidic residues D37, 40, and E43 are represented as sticks, while R98 and 108 involved in the nanoparticle surface anchorage are shown in sticks colored in dark blue.

the signatures of the amino acids as well as amide bands of the protein close to the metal surface. Hence only those proteins can be studied where the region of interest is bound to the metal surface or close to it. This apparent limitation can be circumvented by controlling the orientation of the protein on the metal surface by fusing a metal-seeking short polypeptide chain to the protein at the permissible site of the protein close to the region of interest.<sup>47</sup> Also, a protein can be sandwiched between two metal surface to nullify the distance-dependent effect.<sup>48</sup> In the case of protein C, structure-guided analysis of C protein dimer (generated using the crystal structure of the Mor protein from bacteriophage Mu, PDB ID 1RR7, see Supporting Information for details) indicated that it could be interacting with citrate-reduced silver nanoparticle through basic residues Arg 98 and Arg 108, from the two positively charged patches located at helix 4, 5, and 6 of each monomer (Figure 2). This mode of interaction with the Ag nanoparticle orients the 2-fold axis of C dimer perpendicular to the citrated surface of the nanoparticle, allowing a constellation of basic residues, namely, Arg 87, 105, and 120, which are crucial for C protein–DNA interaction<sup>49</sup>

remain solvent exposed and free. The proposed interaction model was further supported by electrophoretic mobility shift assay (EMSA) studies elucidating the DNA binding ability of C protein in the presence of the nanoparticle (see Figure S3, Supporting Information). Notably, SERS does not enhance all the Raman active modes of a molecule. According to the surface selection rule,<sup>50,51</sup> SERS enhances only those modes with a component of vibrational amplitude perpendicular to the metal surface, leaving out the component parallel to the surface.<sup>52</sup>

**Band Assignment of C Protein.** To assess the conformational changes in C protein by SERS, we relied on the band assignment carried out for proteins studied by SERS previously.<sup>26,53–56</sup> As reported in earlier analyses,<sup>19,26,53</sup> SERS study of C protein also showed a major spectral contribution from the aromatic amino acid residues due to the strong polarizability of the  $\pi$  electrons in the presence of the electric field emanating from the silver surface.<sup>53,57</sup> Figure 2 shows a schematic of the plausible orientation of the protein attached on the silver nanoparticle and the relative distances as a guide to the eye to understand these assignments (Table 1). We have

**Table 1. Assignments of Raman Bands in the SERS Spectra of Protein C and Mutant Protein C with and without Mg<sup>2+</sup> from the Literature<sup>26,53–56</sup>**

protein C	protein C + 5 mM Mg <sup>2+</sup>	mutant C	mutant C + 5 mM Mg <sup>2+</sup>	SERS band assignments <sup>a</sup>
625	625	624	624	Phe ( $\nu_{6b}$ )
639	639	639	639	CC skeletal stretch/ $\nu(C-S)$ /ring deformation (Phe/Tyr)
721	721	719	719	$\tau(C-OH)$
763	764	763	767	Trp <sup>W19</sup>
822	822	822	822	Tyr
848	846	844	847	Tyr
929	929	929	927	$\nu(C-COO^-)$
1011	1010	1010	1010	Phe( $\nu_{12}$ )
1144	1141			ring stretch/ $\nu_{as}(C_\alpha CN)$
		1175	1176	Tyr and/or Phe( $\nu_{9a}$ )
1217	1212	1218	1208	Phe ( $\nu_{7a}$ )
1248	1248	1254	1251	Trp <sup>W10</sup> and/or amide III (random coil)
1269	1269	1269	1269	$\delta(CC_\alpha H)$ and/or amide III ( $\alpha$ -helix)
1345	1343	1345	1345	Trp <sub>W7</sub> and/or $\delta(CH)$
1386	1389	1386	1385	$\nu_s(COO^-)$
1408	1402	1405	1407	$\nu_s(COO^-)$
1449	1445	1445	1445	$\delta(CH_2)$
1459	1462	1463	1462	$\delta(CH_2)$
1496	1499	1495	1502	Trp
1580	1582	1580	1582	$\nu_{as}(COO^-)$ , Trp <sup>W2</sup> , and/or Phe
1621	1621	1618	1618	amide I ( $\alpha$ -helix)

<sup>a</sup> $\nu$ , stretching;  $\delta$ , deformation; s, symmetric; as, asymmetric.

drawn an imaginary 2 nm layer over the silver nanoparticle to visualize the contributions to the SERS spectra from various moieties, provided the selection rules are satisfied for these moieties. Similar representations have been used for assignments in the previous literature.<sup>47,58</sup>

**SER Spectrum of C Protein without Mg<sup>2+</sup>. Amide Vibration.** The amide I mode consists of the C=O stretching vibration with a small admixture of the N-H bending, while amide II is a combination of the N-H bending and C-N stretching. The amide III mode is also a mixture, but with a different sign in the combination of the coordinates. These modes are highly sensitive to the secondary structure of the protein.<sup>1</sup> In the absence of Mg<sup>2+</sup>, we observed amide I and III vibrations of C protein. The band at 1269 cm<sup>-1</sup> is assigned as amide III band, corresponding to the  $\alpha$ -helical secondary structure of the protein. This band has an overlap with  $\delta(CC_\alpha H)$  vibration (see Figure 4). The shoulder at 1248 cm<sup>-1</sup> can be assigned as amide III band, corresponding to the part of the protein in disordered loop or random coil state. The band at 1621 cm<sup>-1</sup> is assigned as amide I, which again corresponds to the  $\alpha$ -helical regions of the protein. The appearance of this band toward the lower wavenumber range of amide band was also observed by several other proteins, such as, lysozyme, soybean trypsin inhibitor (STI),<sup>53</sup> and p300.<sup>19</sup>

In order to confirm our amide band assignment, we carried out SERS of deuterated C protein in the presence of Mg<sup>2+</sup>. In normal Raman experiment this method is commonly used to assign bands, particularly for amide modes.<sup>59,60</sup> The hydrogen to deuterium (H/D) exchange method replaces accessible and exchangeable hydrogens of the protein, both in the main chain amide group N-H as well as the side chain containing acidic groups like OH, NH, and SH.<sup>59,61</sup> In deuterated C protein we observed the appearance of a band as a shoulder around 1600 cm<sup>-1</sup>, which we assigned as amide I' band due to deuterium exchange. As mentioned, amide I band is a mixture of N-H bending and C=O stretching. Because of deuterium exchange,

N-D bending frequency shifts below 1000 cm<sup>-1</sup> and decouples from C=O stretch. This decoupling results in a small red shift of the mode, which is designated as amide I'.<sup>1</sup> Since typically not all amide protons are exchanged with deuterium, both amide I and amide I' exists in a deuterated protein.<sup>1</sup> The amide I' band is generally red-shifted by 10–20 cm<sup>-1</sup> compared to the amide I band,<sup>59,62</sup> as also observed in our experiment (Figure 3). Given

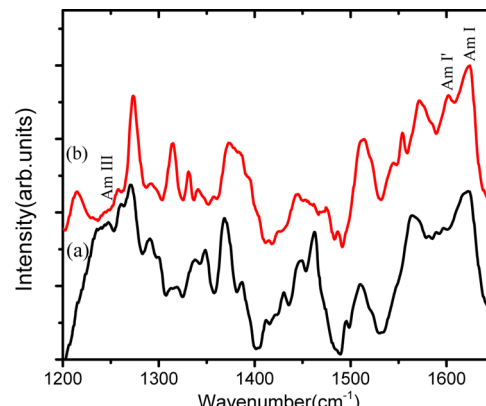


**Figure 3.** SER spectra of C protein in the presence of Mg<sup>2+</sup> (a) in H<sub>2</sub>O and (b) in D<sub>2</sub>O. In the deuterated C protein a band at 1600 cm<sup>-1</sup> appears as a shoulder, which is assigned as amide I'. A band at around 1245 cm<sup>-1</sup> is diminished indicating the plausible contribution from amide III vibration.

the observed magnitude of the band shift to be around 20 cm<sup>-1</sup>, we could also rule out the possibility that the band is due to Trp residue, which is known to undergo only a small red shift of 4 cm<sup>-1</sup>.<sup>59</sup> This distinct nature of the band's sensitivity to H/D exchange confirms our assignment of amide I. Although amide III band is also sensitive to H/D exchange and shifts to around 950 cm<sup>-1</sup>, the presence of other strong bands in the region around 950 cm<sup>-1</sup> prevented us from its unambiguous detection.

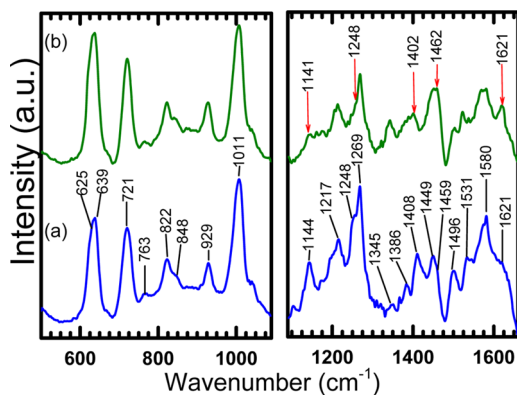


**Figure 4.** Surface-enhanced Raman spectra of wild-type C protein in the (a) absence and (b) presence of Mg<sup>2+</sup>. Arrows (red) show the change in spectra occurred after the addition of Mg<sup>2+</sup>. Spectra are split into two panels as different scales are used for the Y-axis for the clarity of representation.

However, we do observe a reduction in the intensity of the amide III region around 1245 cm<sup>-1</sup> upon deuteration. Our assignment is also supported from literature of both normal Raman<sup>63</sup> and SERS.<sup>53</sup> Upon deuteration some other bands change their positions and intensities. Similar changes were observed both in normal Raman<sup>59</sup> and SERS.<sup>26</sup> Because of H/D exchange the nature of the mode may change,<sup>59</sup> which may affect the observed changes of the bands.

**Aromatic Side-Chain Vibration.** SERS spectra of proteins are dominated by amino acids with aromatic side chain because of their affinity to the metal surface. This has been shown in the spectra of bovine serum albumin (BSA), lysozyme, and cytochrome C.<sup>53,55,64</sup> In this study, we have found significant contribution from the substituted rings of Trp, Tyr, and Phe. Phe ring breathing vibrations  $\nu_{\text{6b}}$ ,  $\nu_{\text{12}}$ , and  $\nu_{\text{7a}}$  were observed at 625, 1011, and 1217 cm<sup>-1</sup>, respectively, owing to the proximity of the Phe residue to the surface. This is rather expected, as Phe 95 is located near the basic patch of the C, involved in nanoparticle adherence. The SERS bands at 763, 1248, and 1580 cm<sup>-1</sup> are due to the Trp indole ring W<sup>19</sup>, W<sup>10</sup>, and W<sup>2</sup> vibrations, respectively. The appearance of these bands due to Trp (residue no. 30) is consistent with our assumption of the protein lying flat with its 2-fold dimerization axis perpendicular to the silver surface. The bands at 639, 822, and 848 cm<sup>-1</sup> are due to Tyr residues. Tyr residues 92, 107, and 115 are located near the positive patch of the C protein, while Tyr 75 is present near the Mg<sup>2+</sup> binding domain. The characteristic doublet band, which reflects the environmental conditions around different Tyr residues, is commonly used to determine the ratio of the number of Tyr residues buried to exposed in a protein in normal Raman spectrum.<sup>29,30,65</sup> These peaks represent Fermi doublet arising from a resonance between the ring breathing vibration and the overtone of the out-of-plane ring bend vibration of the para-substituted phenyl ring in Tyr.<sup>66</sup> Notably, in the SERS spectrum of C in the absence of Mg<sup>2+</sup>, we observed these bands in the range of 822–848 cm<sup>-1</sup>.

**Aliphatic Side-Chain Vibration.** The appearance of bands at around 929 and 1386–1408 cm<sup>-1</sup> are due to the stretching vibration of C–COO<sup>−</sup> and symmetric stretching of COO<sup>−</sup>. These bands, carrying the signature of the carboxyl groups from either side chain of acidic residues such as Asp, Glu, or the carboxy-terminal of a protein, are common features observed in SERS spectra of all the proteins that get adsorbed on the silver

surface.<sup>19,53</sup> As evident from Figure 2, several acidic residues, such as Asp 88 and 89 from helix 4, Glu 101 and 102 from helix 5, and Mg<sup>2+</sup> interacting residues Asp 37 and 40 from helix 1 of at least one monomer, as well as the terminal carboxyl of C protein lie in the vicinity of the silver surface. The band at 1144 cm<sup>-1</sup> is assigned to  $\nu_{\text{as}}(\text{C}_\alpha\text{CN})$  vibration. Deformation mode of CH<sub>2</sub> is also seen at 1449 and 1459 cm<sup>-1</sup>.

**Spectral Changes in the Presence of Mg<sup>2+</sup>.** In the case of SERS, conformational changes in the protein would also lead to differences in the alignment of the amino acid residues adsorbed to the metal surface, leading to the appearance or disappearance of some bands. To study conformational changes in trans-activator protein C in the presence of the Mg<sup>2+</sup>,<sup>27,28</sup> only the well-established normal Raman bands were used as markers. The intensity of the band at 1011 cm<sup>-1</sup> (Phe( $\nu_{12}$ )) was used for normalizing the spectra in order to study the changes occurring in C protein spectra induced by the addition of metal ion. This band is known to be insensitive to the environmental or structural change.<sup>67–69</sup> Moreover, since the band has A<sub>1</sub> symmetry, its intensity should be independent of the change in the protein's orientation on the metal surface following the conformational transitions.<sup>50</sup> The addition of Mg<sup>2+</sup> gives rise to an increase of amide I band intensity but a decrease in intensity of amide III band (Table 1). This spectral alteration could be due to the (i) change in distance of the polypeptide backbone from the silver surface, (ii) change in the orientation of the secondary structural elements of C protein with respect to the silver surface, or (iii) Mg<sup>2+</sup>-induced conformational transition in C protein triggering an increase in alpha helical content. According to Dieringer et al.,<sup>70</sup> the intensity of a peak goes down to one tenth of its initial value at a distance of about 30 Å. As demonstrated in a later section, Mg<sup>2+</sup> binding induces rather a small root-mean-square (rms) deviation of ~1.5 Å in the overall structure. It does not cause any drastic local structural alteration in helices 5 and 6, involved in adherence to the silver surface. Therefore, it is highly unlikely that the observed spectral changes are due to the change in distance from nanoparticle surface. Since the amide band corresponds to the vibration of a series of molecular oscillators, reason (ii) is only valid if there is a large tilt of the existing  $\alpha$ -helices, which would be a contradiction with the predictions from molecular modeling. The CD spectral changes recorded earlier<sup>27,28</sup> indicated a change in helical content of C protein induced by Mg<sup>2+</sup> binding, which corroborates well with reason (iii). The increase in the intensity of the amide I band at the expense of amide III is caused by the structural transitions in the C protein, resulting in higher helical content, induced by metal binding. Similar changes in the intensities of the amide bands in SERS has been used to show the change in secondary structures in earlier studies.<sup>40,71</sup> We observed a decrease in the intensity of the 1144 cm<sup>-1</sup> ( $\nu_{\text{as}}(\text{C}_\alpha\text{CN})$ ), which can be attributed to the change in backbone conformation. The change in secondary and tertiary structural elements of C protein involves formation of a stronger hydrogen bond network, which dampens the asymmetric vibration, hence the decrease in intensity. Ferrari et al.<sup>63</sup> used  $\nu(\text{C}-\text{N})$  as a Raman marker band to visualize conformational changes. Among other spectral changes observed in C protein in the presence of Mg<sup>2+</sup> is the shift of the band corresponding to  $\nu_s(\text{COO}^-)$  from 1408 to 1402 cm<sup>-1</sup>. The shift could be caused by the coordination of the Mg<sup>2+</sup> ion with the carboxyl oxygen of (–COO<sup>−</sup>) from the acidic residues involved in metal binding, similar to the ligand induced red shift observed by Ferrari et al.<sup>63</sup> The presence of Mg<sup>2+</sup> increases the positional separation of the peaks between the symmetric and asymmetric COO<sup>−</sup> vibrations, which can be attributed to the involvement of one of the O

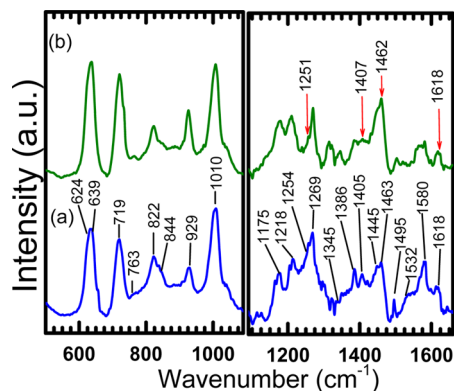


**Figure 5.** Surface-enhanced Raman spectrum of mutant C protein in the (a) absence and (b) presence of Mg<sup>2+</sup>. Unlike the wild-type C protein, the peaks (red arrow) showed no substantial changes in the mutant C protein upon Mg<sup>2+</sup> addition. Spectra are split into two panels as different scales are used for the Y-axis for the clarity of representation.

atom(s) in metal binding.<sup>72</sup> Similarly, the increase of 1345 cm<sup>-1</sup> band corresponding to the Trp residues could be attributed to the conformational changes in C protein altering the orientation of the contributing Trp(s). Further, the band at 1459 cm<sup>-1</sup>, which appears as a shoulder, increased in intensity in the presence of Mg<sup>2+</sup>. This band is due to CH<sub>2</sub> deformation and is a signature of hydrophobic interactions.<sup>73,74</sup> Therefore, this change can be

ascribed to the increased hydrophobic interactions arising due to the tertiary structural transition in the presence of Mg<sup>2+</sup>.

**SER Spectrum of Mutated C Protein.** In order to verify the above analysis, similar studies were carried out with mutant C protein D40N, compromised in Mg<sup>2+</sup> binding. In the SERS spectra of the mutant, we observed very little change in the intensity of the amide I and III bands upon the addition of Mg<sup>2+</sup> (see arrows in Figure 5). Further, because of the inability of the mutant protein to bind Mg<sup>2+</sup>, the band at 1405 cm<sup>-1</sup> corresponding to the COO<sup>-</sup> group did not shift appreciably. Unlike wild-type C, no significant change in the intensity due to δ(CH<sub>2</sub>) was observed. An increase in intensity of 1345 cm<sup>-1</sup> can be attributed to altered orientation(s) of Trp side chain, possibly caused by nonspecific and transitional interaction with metal ion.

To better understand the structural transitions occurring in the transactivator C protein detected by SERS, the spectral data were correlated with the three-dimensional model of C. In the model of the C protein dimer–Mg<sup>2+</sup> complex, each monomer is shown to bind one metal ion. The metal binding site of C protein is composed of a negatively charged patch at dimeric interface, rich in acidic residues, such as Asp 37 and 40 and Glu 43 from one monomer and Asp 89 from the other. The interaction of acidic residues D40 and D37 with Mg<sup>2+</sup>, at the site of metal binding, is elucidated in Figure 6. Structural superimposition of energy minimized molecular models of C dimers, generated in the absence and presence of the bound Mg<sup>2+</sup> ions showed an rms

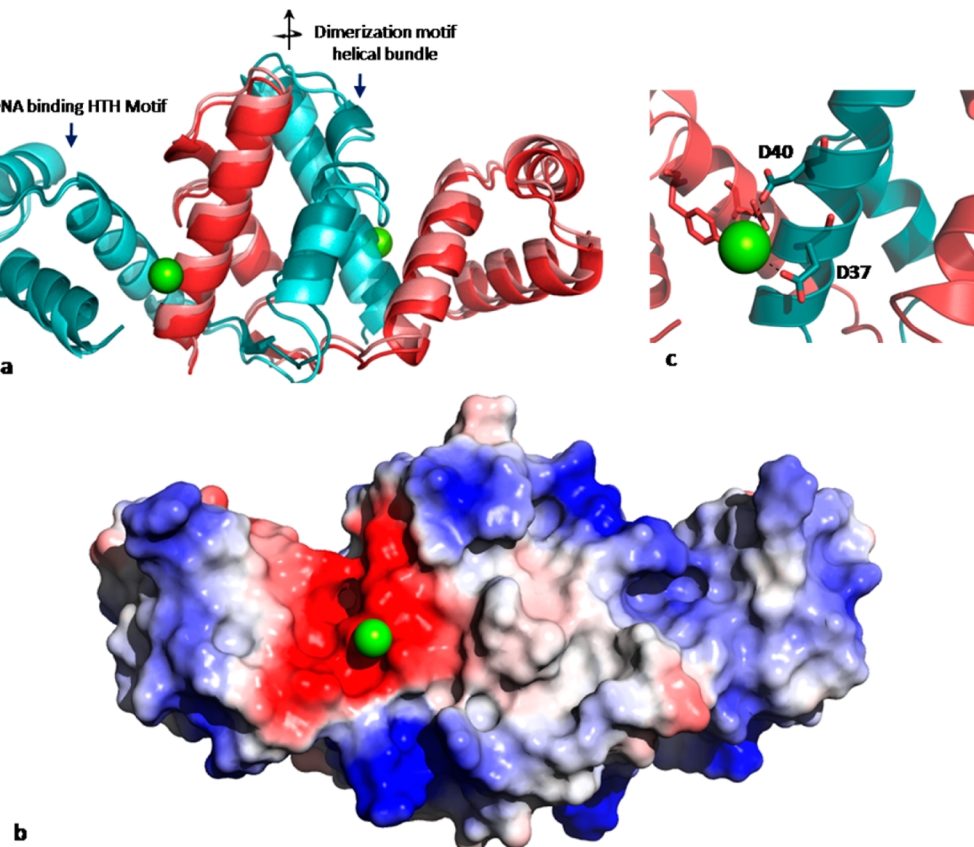


**Figure 6.** Molecular modeling of C protein for structural elucidation of Mg<sup>2+</sup> ion binding and induced conformational changes. C protein monomers assemble into dimeric form following a 2-fold rotational symmetry. Monomer chains A and B are displayed in teal and red, respectively. (a) Three-dimensional structural alignment of energy minimized C protein dimer models, in the presence and absence (displayed in lighter shades of teal and red) of Mg<sup>2+</sup> ions. (b) Representation of the surface electrostatics of C-dimer, displaying the Mg<sup>2+</sup> ion binding site. The binding site harbors a negatively charged patch, formed by acidic amino acids, such as D37, D40, and E43 from one monomer and D89 from other. (C) Interaction of metal ion with acidic residues D37 and D40. Color codes corresponding to residue charges (blue, positive; red, negative).

deviation of about 1.5 Å (Figure 6). This reveals an overall structural change in C protein upon metal ion binding, consistent with the spectral changes observed in SERS. The model also showed that the single Trp residue contributing to the band at 1345 cm<sup>-1</sup> is located at a helix-loop boundary (Figure 2b) and hence prone to minute structural perturbation caused even by the nonspecific metal interaction(s). The inherent transient nature of the Trp environment suggests its exclusion as a marker from this study. However, the conformational change in the C-dimer is of crucial implications, as it leads to high affinity DNA binding by the protein followed by transcription activation.<sup>28,49</sup> Further, our study also establishes Mg<sup>2+</sup> interacting residue D40 as an important perturbation point in the whole process, as mutation of D40 to N abolishes the protein's ability to undergo allosteric transition into the active state upon Mg<sup>2+</sup> binding.

## CONCLUSIONS

In summary, we have shown that the SERS could be used as a tool to study the secondary as well as tertiary structural changes in proteins. The increase in alpha helical content and the concomitant fall in random coil observed by SERS suggest the applicability of the method to study secondary structural transitions. The changes of SERS band intensities associated with altered orientations of aliphatic and aromatic side chains and conformational changes in the peptide backbone indicate structural changes in C protein upon Mg<sup>2+</sup> binding. The changes caused by the coordinate interactions between side chain carboxyl groups from acidic residues of C and bound Mg<sup>2+</sup> are detected, which act as a trigger for the allosteric transition. As in the case of transactivator C, SERS can be potentially applied to monitor conformational changes in a diverse class of regulatory protein with further modifications. A large number of DNA transaction proteins undergo conformational changes upon ligand binding in order to carry out their regulatory functions. SERS does not require a label to be attached to the protein for detecting conformational changes. Most of the regulatory proteins are indeed found in low concentration in the cells, and hence, SERS could be envisioned as a useful future technique for imaging applications. As shown previously with peptides,<sup>75</sup> our SERS-based exploration of the ligand induced conformational changes in C protein also demonstrates the possibility of its application as a highly sensitive nanoscale detection method of biological or chemical stimuli *in vitro*. SERS, therefore, stands as an attractive and powerful biophysical tool to explore various biological processes, expanding the feasibility of application into systems with minute sample availabilities.

## ASSOCIATED CONTENT

### Supporting Information

Absorption spectrum, DLS measurement, and TEM image of the Ag nanoparticle, SERS of buffer, computational study, DNA binding study, and aggregation study of Ag np in the presence of MgCl<sub>2</sub>. This material is available free of charge via the Internet at <http://pubs.acs.org>.

## AUTHOR INFORMATION

### Corresponding Authors

\*(C.N.) E-mail: cbhas@jncasr.ac.in.

\*(V.N.) E-mail: vraj@mcb.iisc.ernet.in.

### Present Address

<sup>II</sup>(P.K.) Division of Physics and Chemistry, Indian Institute of Science Education and Research, Pune 411008, India.

## Author Contributions

<sup>1</sup>The manuscript was written through contributions of all authors. All authors have given approval to the final version of the manuscript. These authors contributed equally.

## Notes

The authors declare no competing financial interest.

## ACKNOWLEDGMENTS

P.P.K. and T.B. would like to thank Council of Scientific and Industrial Research, India for Senior Research Fellowship.

## REFERENCES

- (1) Sieber, F.; Hildebrandt, P. *Vibrational Spectroscopy in Life Science*; Wiley-VCH Verlag GmbH & Co. KGaA: Berlin, Germany, 2008.
- (2) Ellis, D. I.; Brewster, V. L.; Dunn, W. B.; Allwood, J. W.; Golovanov, A. P.; Goodacre, R. Fingerprinting Food: Current Technologies for the Detection of Food Adulteration and Contamination. *Chem. Soc. Rev.* **2012**, *41*, 5706–5727.
- (3) González, A.; Garrigues, S.; Armenta, S.; de la Guardia, M. Headspace-Liquid Phase Microextraction for Attenuated Total Reflection Infrared Determination of Volatile Organic Compounds at Trace Levels. *Anal. Chem.* **2010**, *82*, 3045–3051.
- (4) Jarvis, R. M.; Brooker, A.; Goodacre, R. Surface-Enhanced Raman Spectroscopy for Bacterial Discrimination Utilizing a Scanning Electron Microscope with a Raman Spectroscopy Interface. *Anal. Chem.* **2004**, *76*, 5198–5202.
- (5) Lim, D. K.; Jeon, K. S.; Kim, H. M.; Nam, J. M.; Suh, Y. D. Nanogap-Engineerable Raman-Active Nanodumbbells for Single-Molecule Detection. *Nat. Mater.* **2010**, *9*, 60–67.
- (6) Qian, X. M.; Nie, S. M. Single-Molecule and Single-Nanoparticle SERS: From Fundamental Mechanisms to Biomedical Applications. *Chem. Soc. Rev.* **2008**, *37*, 912–920.
- (7) Brus, L. Noble Metal Nanocrystals: Plasmon Electron Transfer Photochemistry and Single-Molecule Raman Spectroscopy. *Acc. Chem. Res.* **2008**, *41*, 1742–1749.
- (8) Kleinman, S. L.; Ringe, E.; Valley, N.; Wustholz, K. L.; Phillips, E.; Scheidt, K. A.; Schatz, G. C.; Van Duyne, R. P. Single-Molecule Surface-Enhanced Raman Spectroscopy of Crystal Violet Isotopologues: Theory and Experiment. *J. Am. Chem. Soc.* **2011**, *133*, 4115–4122.
- (9) Ahijado-Guzmán, R.; Gómez-Puertas, P.; Alvarez-Puebla, R. A.; Rivas, G.; Liz-Marzáñ, L. M. Surface-Enhanced Raman Scattering-Based Detection of the Interactions between the Essential Cell Division FtsZ Protein and Bacterial Membrane Elements. *ACS Nano* **2012**, *6*, 7514–7520.
- (10) Abdali, S.; De Laere, B.; Poulsen, M.; Grigorian, M.; Lukanić, E.; Klingelhöfer, J. Toward Methodology for Detection of Cancer-Promoting S100A4 Protein Conformations in Subnanomolar Concentrations Using Raman and SERS. *J. Phys. Chem. C* **2010**, *114*, 7274–7279.
- (11) Barhoumi, A.; Halas, N. J. Label-Free Detection of DNA Hybridization Using Surface Enhanced Raman Spectroscopy. *J. Am. Chem. Soc.* **2010**, *132*, 12792–12793.
- (12) Kang, T.; Yoo, S. M.; Yoon, I.; Lee, S. Y.; Kim, B. Patterned Multiplex Pathogen DNA Detection by Au Particle-on-Wire SERS Sensor. *Nano Lett.* **2010**, *10*, 1189–1193.
- (13) Ochsenkuhn, M. A.; Campbell, C. J. Probing Biomolecular Interactions Using Surface Enhanced Raman Spectroscopy: Label-Free Protein Detection Using a G-Quadruplex DNA Aptamer. *Chem. Commun.* **2010**, *46*, 2799–2801.
- (14) Papadopoulou, E.; Bell, S. E. J. Label-Free Detection of Single-Base Mismatches in DNA by Surface-Enhanced Raman Spectroscopy. *Angew. Chem., Int. Ed.* **2011**, *50*, 9058–9061.
- (15) Kneipp, K.; Kneipp, H.; Kneipp, J. Surface-Enhanced Raman Scattering in Local Optical Fields of Silver and Gold Nanoaggregates From Single-Molecule Raman Spectroscopy to Ultrasensitive Probing in Live Cells. *Acc. Chem. Res.* **2006**, *39*, 443–450.

- (16) Moore, B. D.; Stevenson, L.; Watt, A.; Flitsch, S.; Turner, N. J.; Cassidy, C.; Graham, D. Rapid and Ultra-Sensitive Determination of Enzyme Activities Using Surface-Enhanced Resonance Raman Scattering. *Nat. Biotechnol.* **2004**, *22*, 1133–1138.
- (17) Bonham, A. J.; Braun, G.; Pavel, I.; Moskovits, M.; Reich, N. O. Detection of Sequence-Specific Protein-DNA Interactions via Surface Enhanced Resonance Raman Scattering. *J. Am. Chem. Soc.* **2007**, *129*, 14572–14573.
- (18) Graham, D.; Mallinder, B. J.; Smith, W. E. Surface-Enhanced Resonance Raman Scattering as a Novel Method of DNA Discrimination. *Angew. Chem., Int. Ed.* **2000**, *39*, 1061–1063.
- (19) Pavan Kumar, G. V.; Ashok Reddy, B. A.; Arif, M.; Kundu, T. K.; Narayana, C. Surface-Enhanced Raman Scattering Studies of Human Transcriptional Coactivator P300. *J. Phys. Chem. B* **2006**, *110*, 16787–16792.
- (20) Mantelingu, K.; Kishore, A. H.; Balasubramanyam, K.; Kumar, G. V. P.; Altaf, M.; Swamy, S. N.; Selvi, R.; Das, C. I.; Narayana, C.; Rangappa, K. S.; et al. Activation of P300 Histone Acetyltransferase by Small Molecules Altering Enzyme Structure: Probed by Surface-Enhanced Raman Spectroscopy. *J. Phys. Chem. B* **2007**, *111*, 4527–4534.
- (21) Mantelingu, K.; Reddy, B. A. A.; Swaminathan, V.; Kishore, A. H.; Siddappa, N. B.; Kumar, G. V. P.; Nagashankar, G.; Natesh, N.; Roy, S.; Sadhale, P. P.; et al. Specific Inhibition of p300-HAT Alters Global Gene Expression and Represses HIV Replication. *Chem. Biol.* **2007**, *14*, 645–657.
- (22) Kundu, P. P.; Narayana, C. Raman Based Imaging in Biological Application: A Perspective. *J. Med. Allied Sci.* **2012**, *2*, 41–48.
- (23) Habuchi, S.; Cotlet, M.; Gronheid, R.; Dirix, G.; Michiels, J.; Vanderleyden, J.; De Schryver, F. C.; Hofkens, J. Single-Molecule Surface Enhanced Resonance Raman Spectroscopy of the Enhanced Green Fluorescent Protein. *J. Am. Chem. Soc.* **2003**, *125*, 8446–8447.
- (24) Han, X. X.; Huang, G. G.; Zhao, B.; Ozaki, Y. Label-Free Highly Sensitive Detection of Proteins in Aqueous Solutions Using Surface-Enhanced Raman Scattering. *Anal. Chem.* **2009**, *81*, 3329–3333.
- (25) Han, X. X.; Zhao, B.; Ozaki, Y. Surface-Enhanced Raman Scattering for Protein Detection. *Anal. Bioanal. Chem.* **2009**, *394*, 1719–1727.
- (26) Kumar, G. V. P.; Selvi, R.; Kishore, A. H.; Kundu, T. K.; Narayana, C. Surface-Enhanced Raman Spectroscopic Studies of Coactivator-Associated Arginine Methyltransferase 1. *J. Phys. Chem. B* **2008**, *112*, 6703–6707.
- (27) De, A.; Ramesh, V.; Mahadevan, S.; Nagaraja, V. Mg<sup>2+</sup> Mediated Sequence-Specific Binding of Transcriptional Activator Protein C of Bacteriophage Mu to DNA. *Biochemistry* **1998**, *37*, 3831–3838.
- (28) Swapna, G.; Saravanan, M.; Nagaraja, V. Conformational Changes Triggered by Mg<sup>2+</sup> Mediate Transactivator Function. *Biochemistry* **2009**, *48*, 2347–2354.
- (29) Anzenbacher, P.; Mojzes, P.; Baumruk, V.; Amler, E. Changes in Na<sup>+</sup>,K<sup>+</sup>-ATPase Structure Induced by Cation Binding Approach by Raman Spectroscopy. *FEBS Lett.* **1992**, *312*, 80–82.
- (30) Nabiev, I. R.; Dzhandzhugazyan, K. N.; Efremov, R. G.; Modyanov, N. N. Binding of Monovalent Cations Induces Large Changes in the Secondary Structure of Na<sup>+</sup>,K<sup>+</sup>-ATPase as Probed by Raman Spectroscopy. *FEBS Lett.* **1988**, *236*, 235–239.
- (31) Nielsen, C. H.; Abdali, S.; Lundbæk, J. A.; Cornelius, F. Raman Spectroscopy of Conformational Changes in Membrane-Bound Sodium Potassium ATPase. *Spectroscopy* **2007**, *22*, 52–63.
- (32) Asher, S. A. UV Resonance Raman Spectroscopy for Analytical, Physical, and Biophysical Chemistry. Part 1. *Anal. Chem.* **1993**, *65*, 59A–66A.
- (33) JiJi, R. D.; Balakrishnan, G.; Hu, Y.; Spiro, T. G. Intermediacy of Poly (L-Proline) II and  $\beta$ -Strand Conformations in Poly (L-Lysine)  $\beta$ -Sheet Formation Probed by Temperature-Jump/UV Resonance Raman Spectroscopy. *Biochemistry* **2005**, *45*, 34–41.
- (34) Asher, S. A.; Ianoul, A.; Mix, G.; Boyden, M. N.; Karnoup, A.; Diem, M.; Schweitzer-Stenner, R. Dihedral  $\gamma$  Angle Dependence of the Amide III Vibration: A Uniquely Sensitive UV Resonance Raman Secondary Structural Probe. *J. Am. Chem. Soc.* **2001**, *123*, 11775–11781.
- (35) Chi, Z.; Asher, S. A. UV Resonance Raman Determination of Protein Acid Denaturation: Selective Unfolding of Helical Segments of Horse Myoglobin. *Biochemistry* **1998**, *37*, 2865–2872.
- (36) Ahmed, Z.; Beta, I. A.; Mikhonin, A. V.; Asher, S. A. UV-Resonance Raman Thermal Unfolding Study of Trp-Cage Shows That It Is Not a Simple Two-State Miniprotein. *J. Am. Chem. Soc.* **2005**, *127*, 10943–10950.
- (37) Jayaraman, V.; Rodgers, K. R.; Mukerji, I.; Spiro, T. G. Hemoglobin Allostery: Resonance Raman Spectroscopy of Kinetic Intermediates. *Science* **1995**, *269*, 1843–1848.
- (38) Feng, M.; Tachikawa, H. Surface-Enhanced Resonance Raman Spectroscopic Characterization of the Protein Native Structure. *J. Am. Chem. Soc.* **2008**, *130*, 7443–7448.
- (39) Singhal, K.; Kalkan, A. K. Surface-Enhanced Raman Scattering Captures Conformational Changes of Single Photoactive Yellow Protein Molecules under Photoexcitation. *J. Am. Chem. Soc.* **2009**, *132*, 429–431.
- (40) Choi, I.; Huh, Y.; Erickson, D. Ultra-Sensitive, Label-Free Probing of the Conformational Characteristics of Amyloid Beta Aggregates With a SERS Active Nanofluidic Device. *Microfluid. Nanofluid.* **2012**, *12*, 663–669.
- (41) Ramesh, V.; De, A.; Nagaraja, V. Engineering Hyperexpression of Bacteriophage-Mu C-Protein by Removal of Secondary Structure at the Translation Initiation Region. *Protein Eng.* **1994**, *7*, 1053–1057.
- (42) Lee, P. C.; Meisel, D. Adsorption and Surface-Enhanced Raman of Dyes on Silver and Gold Sols. *J. Phys. Chem.* **1982**, *86*, 3391–3395.
- (43) Kumar, G. V. P.; Narayana, C. Adapting a Fluorescence Microscope to Perform Surface Enhanced Raman Spectroscopy. *Curr. Sci. India* **2007**, *93*, 778–781.
- (44) Ramesh, V.; Nagaraja, V. Sequence-Specific DNA Binding of the Phage Mu C Protein: Footprinting Analysis Reveals Altered DNA Conformation Upon Protein Binding. *J. Mol. Biol.* **1996**, *260*, 22–33.
- (45) Basak, S.; Nagaraja, V. DNA Unwinding Mechanism for the Transcriptional Activation of momP1 Promoter by the Transactivator Protein C of Bacteriophage Mu. *J. Biol. Chem.* **2001**, *276*, 46941–46945.
- (46) Kneipp, K.; Kneipp, H.; Itzkan, I.; Dasari, R. R.; Fed, M. S. Surface-Enhanced Raman Scattering and Biophysics. *J. Phys.: Condens. Matter* **2002**, *14*, R597.
- (47) Sengupta, A.; Thai, C. K.; Sastry, M. S. R.; Matthaei, J. F.; Schwartz, D. T.; Davis, E. J.; Baneyx, F. A Genetic Approach for Controlling the Binding and Orientation of Proteins on Nanoparticles. *Langmuir* **2008**, *24*, 2000–2008.
- (48) Keating, C. D.; Kovaleski, K. M.; Natan, M. J. Protein: Colloid Conjugates for Surface Enhanced Raman Scattering: Stability and Control of Protein Orientation. *J. Phys. Chem. B* **1998**, *102*, 9404–9413.
- (49) Paul, B. D.; Kanhere, A.; Chakraborty, A.; Bansal, M.; Nagaraja, V. Identification of the Domains for DNA Binding and Transactivation Function of C Protein From Bacteriophage Mu. *Proteins* **2003**, *52*, 272–282.
- (50) Hallmark, V. M.; Campion, A. Selection Rules for Surface Raman Spectroscopy: Experimental Results. *J. Chem. Phys.* **1986**, *84*, 2933–2941.
- (51) Moskovits, M. Surface Selection Rules. *J. Chem. Phys.* **1982**, *77*, 4408–4416.
- (52) Yu, Q. M.; Golden, G. Probing the Protein Orientation on Charged Self-Assembled Monolayers on Gold Nanohole Arrays by SERS. *Langmuir* **2007**, *23*, 8659–8662.
- (53) Podstawkwa, E.; Ozaki, Y.; Proniewicz, L. M. Adsorption of S-S Containing Proteins on a Colloidal Silver Surface Studied by Surface-Enhanced Raman Spectroscopy. *Appl. Spectrosc.* **2004**, *58*, 1147–1156.
- (54) Grabbe, E. S.; Buck, R. P. Surface-Enhanced Raman Spectroscopic Investigation of Human Immunoglobulin G Adsorbed on a Silver Electrode. *J. Am. Chem. Soc.* **1989**, *111*, 8362–8366.
- (55) Chen, M. C.; Lord, R. C. Laser-Excited Raman Spectroscopy of Biomolecules. VIII. Conformational Study of Bovine Serum Albumin. *J. Am. Chem. Soc.* **1976**, *98*, 990–992.
- (56) Chumanov, G. D.; Efremov, R. G.; Nabiev, I. R. Surface-Enhanced Raman Spectroscopy of Biomolecules. Part I. Water-Soluble Proteins, Dipeptides and Amino Acids. *J. Raman Spectrosc.* **1990**, *21*, 43–48.

- (57) Podstawka, E.; Ozaki, Y.; Proniewicz, L. M. Part I: Surface-Enhanced Raman Spectroscopy Investigation of Amino Acids and Their Homodipeptides Adsorbed on Colloidal Silver. *Appl. Spectrosc.* **2004**, *58*, 570–580.
- (58) Pavel, I.; McCarney, E.; Elkhaled, A.; Morrill, A.; Plaxco, K.; Moskovits, M. Label-Free SERS Detection of Small Proteins Modified to Act as Bifunctional Linkers. *J. Phys. Chem. C* **2008**, *112*, 4880–4883.
- (59) Overman, S. A.; Thomas, G. J. Amide Modes of the  $\alpha$ -Helix: Raman Spectroscopy of Filamentous Virus fd Containing Peptide  $^{13}\text{C}$  and  $^2\text{H}$  Labels in Coat Protein Subunits. *Biochemistry* **1998**, *37*, 5654–5665.
- (60) Tuma, R.; Prevelige, P. E.; Thomas, G. J. Mechanism of Capsid Maturation in a Double-Stranded DNA Virus. *Proc. Natl. Acad. Sci. U.S.A.* **1998**, *95*, 9885–9890.
- (61) Barth, A.; Zscherp, C. What Vibrations Tell Us About Proteins. *Q. Rev. Biophys.* **2002**, *35*, 369–430.
- (62) Tu, A. T. *Spectroscopy of Biological Systems. Advances in Spectroscopy*; Wiley: Chichester, U.K., 1986; Vol. 13.
- (63) Ferrari, D.; Diers, J. R.; Bocian, D. F.; Kaarsholm, N. C.; Dunn, M. F. Raman Signatures of Ligand Binding and Allosteric Conformation Change in Hexameric Insulin. *Biopolymers* **2001**, *62*, 249–260.
- (64) Cotton, T. M.; Schultz, S. G.; Van Duyne, R. P. Surface-Enhanced Resonance Raman Scattering From Cytochrome C and Myoglobin Adsorbed on a Silver Electrode [21]. *J. Am. Chem. Soc.* **1980**, *102*, 7960–7962.
- (65) Lippert, J. L.; Lindsay, R. M.; Schultz, R. Laser Raman Characterization of Conformational Changes in Sarcoplasmic Reticulum Induced by Temperature,  $\text{Ca}^{2+}$ , and  $\text{Mg}^{2+}$ . *J. Biol. Chem.* **1981**, *256*, 12411–12416.
- (66) Siamwiza, M. N.; Lord, R. C.; Chen, M. C.; Takamatsu, T.; Harada, I.; Matsuura, H.; Shimanouchi, T. Interpretation of the Doublet at  $850$  and  $830\text{ cm}^{-1}$  in the Raman Spectra of Tyrosyl Residues in Proteins and Certain Model Compounds. *Biochemistry* **1975**, *14*, 4870–4876.
- (67) Li-Chan, E. C.; Qin, L. *The Application of Raman Spectroscopy to the Structural Analysis of Food Protein Networks*; AOCS Press: Champaign, IL, 1998.
- (68) Lord, R. C.; Yu, N. T. Laser-Excited Raman Spectroscopy of Biomolecules: I. Native Lysozyme and Its Constituent Amino Acids. *J. Mol. Biol.* **1970**, *50*, 509–524.
- (69) Hedegaard, M.; Krafft, C.; Ditzel, H. J.; Johansen, L. E.; Hassing, S.; Popp, J. Discriminating Isogenic Cancer Cells and Identifying Altered Unsaturated Fatty Acid Content as Associated with Metastasis Status, Using K-Means Clustering and Partial Least Squares-Discriminant Analysis of Raman Maps. *Anal. Chem.* **2010**, *82*, 2797–2802.
- (70) Dieringer, J. A.; McFarland, A. D.; Shah, N. C.; Stuart, D. A.; Whitney, A. V.; Yonzon, C. R.; Young, M. A.; Zhang, X.; Van Duyne, R. P. Introductory Lecture Surface Enhanced Raman Spectroscopy: New Materials, Concepts, Characterization Tools, and Applications. *Faraday Discuss.* **2006**, *132*, 9–26.
- (71) Huang, H.; Xie, J.; Liu, X.; Yuan, L.; Wang, S.; Guo, S.; Yu, H.; Chen, H.; Zhang, Y.; Wu, X. Conformational Changes of Protein Adsorbed on Tailored Flat Substrates with Different Chemistries. *ChemPhysChem* **2011**, *12*, 3642–3646.
- (72) Deacon, G. B.; Phillips, R. J. Relationships Between the Carbon–Oxygen Stretching Frequencies of Carboxylato Complexes and the Type of Carboxylate Coordination. *Coord. Chem. Rev.* **1980**, *33*, 227–250.
- (73) Li-Chan, E.; Nakai, S.; Hirotsuka, M. Raman Spectroscopy as a Probe of Protein Structure in Food System. In *Protein Structure–Function Relationships in Foods*; Yada, R. Y., Jackman, R. L., Eds.; Chapman and Hall, Inc.: London, U.K., 1994; pp 163–197.
- (74) Herrero, A. M. Raman Spectroscopy for Monitoring Protein Structure in Muscle Food Systems. *Crit. Rev. Food Sci. Nutr.* **2008**, *48*, 512–523.
- (75) Chen, Y.; Cruz-Chu, E. R.; Woodard, J. C.; Gartia, M. R.; Schulten, K.; Liu, L. Electrically Induced Conformational Change of Peptides on Metallic Nanosurfaces. *ACS Nano* **2012**, *6*, 8847–8856.